Highly stable porous cellulose materials to utilize lactic acid

So Hee Kim
Sangmyung University
Sang Wook Kang (swkang@smu.ac.kr)
Sangmyung University https://orcid.org/0000-0001-7211-4064

Research Article

Keywords: Wetting Action, Plascticization Effect, Hydrostatic Treatment, Fourier Transform Infrared Spectroscopy, Thermogravimetric Analysis, Water Flux Measurement

Posted Date: March 1st, 2021

DOI: https://doi.org/10.21203/rs.3.rs-170330/v1

Version of Record: A version of this preprint was published at Cellulose on August 21st, 2021. See the published version at https://doi.org/10.1007/s10570-021-04144-7.

Abstract

In this study, a porous membrane consisting of lactic acid and cellulose acetate was fabricated using a low-cost and pro-environmental process. The wetting action of the lactic acid induced a plasticization effect in the cellulose acetate chain, forming several small pores during the hydrostatic treatment. The surface and cross-section of the membranes were observed using scanning electron microscopy, and the interaction between cellulose acetate and lactic acid was investigated using Fourier transform infrared spectroscopy. Furthermore, thermogravimetric analysis was performed to determine the thermal stability of the membrane and the removal of lactic acid by the hydrostatic treatment. In addition, the optimum composition and performance of the composite were investigated via water flux measurement. Furthermore, the average pore diameter and porosity of the cellulose acetate/lactic acid membrane measured using a porosimeter was 0.38 μm and 65.3%, respectively.

1. Introduction

In fields such as environmental, industrial, and biological, etc., porous membranes are boundless used to solve the problems faced mankind.(1-5) In addition, the membranes which have numerous pores are extensively used to purify contaminated water, separate cathode and anode in battery and separate gas in distillation process.(6-10) Porous membrane can absorb or filter only pollutants out of wastewater, and it can leads to tremendous environmental virtue. Futhermore, in industrial fields, membrane process with porous materials is able to simplify complicate processes including cryogenic distillation, water purification and etc.. Depending on the target application, the materials of the porous substance can be of many types, including polymers, ceramics, and metals. There are several methods for fabricating porous membranes such as surface modification, phase separation, water treatment, electrospinning, and 3D-printing.(11-17) Several researchers take considerable pains to develop low expense and pro-environmental methods for the production of separating membranes. Consequently, tremendous efforts have been devoted by researchers to develop new pro-environmental materials such as green solvents (18)and polymers for the eco-friendly production of porous membranes.

Recently, porous substances are often studied as separating membranes. Sushil Adhikari et al. compared the performance of metal and ceramic membranes for high-purity hydrogen separation.(19) In addition, De-en Jiang et al. proposed the use of porous graphene for gas separation.(20) Furthermore, Xiang Zhu et al. synthesized a porous, fluorescent, triazine framework-based membrane with intrinsic porosity through CO_2 aromatic nitrile trimerization.(21) Pan et al. prepared porous membranes with various wettabilities ranging from superhydrophilic to superhydrophobic, utilizing TiO_2 nanowires for oil/water separation.(22) Zhihua Qiao et al. synthesized metal-induced ordered microporous polymers and coated them on a modified polysulfone to develop a membrane for N_2/CO_2 separation.(23) Min Hu et al. prepared a zeolitic imidazolate framework (ZIF-67) trap-in polystyrene hierarchical porous nanofiber membrane (ZIF-67/PS HPNFM) with high gas permeability to remove particulate matter.(24) Shushan Yuan et al. produced a membrane based on COF, a porous material, and reported the advantages and disadvantages of COF

compared with MOFs.(25) Hence, the use of porous membranes as separators have received increased attention among researchers, and thus, are being developed for further research.

PP or PE are primarily worked as plastic separator in battery(26, 27); however, the low thermostability of these materials may cause safety issues such as battery explosion. Therefore, it is important to develop polymer materials with high thermostability and good efficiency.(28-31) To overcome this limitation, several researchers have devoted numerous effort to develop more efficient polymer materials.(32, 33) In this study, to address this issue, we improved the thermostability of cellulose acetate (CA). The melting point of CA is approximately 256 °C, which is higher than that of PP and PE, indicating its high thermostability. In addition, CA is one of the most generally used polymers because it is inexpensive and pro-environmental.

A former study demonstrated the formation of a straight-type pore in biopolymer membrane using Mg salt.(34) This straight-type pore facilitated the rapid movement of lithium ions, improving the ion conductivity of the membrane. In addition, the membrane was pro-environment and reusable since it was made from CA which is derived from nature. However, the Mg salt used in the study reduced the porosity of the membrane. To address this limitation, in this study, humectants were employed to expand the porosity of the membrane, while ensuring an pro-environmental process. In this study, lactic acid, which is an pro-environmental and cheap humectant was employed. In addition, lactic acid shows high dispersibility owing to its good solvation. The dispersion of lactic acid in biopolymer improves the flexibility of the regions dispersed with lactic acid due to the interaction between the polymer chain and lactic acid. In addition, water pressure was applied to the polymer membrane to increase the generation of pores, thus increasing the porosity of the membrane.

2. Experimental

CA ($(Mn)^{-}$~30,000, Sigma-Aldrich Chemical Co.) and lactic acid (Daejung Chemical & Metals) were utilized as the membrane materials. Acetone (Daejung Chemical & Metals) was employed as the solvent. All materials were employed as received without further treatments.

A 10 wt% neat CA membrane solution was prepared by dissolving 1 g of cellulose acetate ($(Mn)^{-}$~30,000) in acetone/H_2O (8:2 wt/wt ratio). Lactic acid was added into the polymer solution at a mole ratio of 1:0.07. Thereafter, the solution was stirred for 4 h at ordinary temperature. The CA/lactic acid membrane was created on a glass plate with a doctor blade using the free-stand method. The membrane was then dried for 30 min in a thermo-hygrostat at 25 °C and 50% humidity. Subsequently, the dried membranes were placed in a water treatment equipment, and water pressure from 2 to 8 bar was applied to the membranes; the water flux was measured as L/m^2h. The membranes were characterized using scanning electron microscopy (SEM), Fourier transform infrared spectroscopy (FT-IR), thermogravimetric analysis (TGA), and a porosimeter.

3. Result And Discussion

3.1 SEM (Scanning Electron spectroscopy)

SEM was carried out to recognize the superficies and cross-section of the membranes. Fig. 1(a) shows the superficies of the neat CA (pristine) with no applied water pressure. No pores were observed on the superficies of the pristine. Similarly, no pores existed in the 1:0.07 CA/lactic acid composite before the hydrostatic treatment (Fig. 1(b)). In contrast, after the hydrostatic treatment at 8 bar, assemblies of pores were generated on the superficies of the 1:0.07 CA/lactic acid composite, as shown in Fig. 1(c). In addition, as shown in Fig. 1(e), several tiny pores were observed on the surface of the 1:0.07 CA/lactic acid membrane. As shown in Scheme 1, the application of water pressure to the plasticized area removed the lactic acid, thus forming pores in the cellulose polymers. Furthermore, as shown in Fig. 1(f), sponge-like pores were formed in the cross-section of the membrane.

3.2 Infrared spectroscopy (FT-IR)

FT-IR spectroscopy was carried out to identify the interactions between CA and lactic acid. The peak existed at 1750 cm^{-1} can be attributed to the C=O bond in the chains. Figure 2 shows the IR data for the C=O bond of the pristine CA, 1:0.07 CA/lactic acid at 0 bar, and 1:0.07 CA/lactic acid at 8 bar membranes. In Fig. 2, since the change in the shift was small, the peaks were analyzed by deconvolution (Fig. 3). According to Table 1, in the range of 1735–1737 cm^{-1}, the area ratio of the pristine CA was 79.19%, while that of the CA/lactic acid at 0 bar membrane was 86.82%. This indicates that the peak shifted to a lower wavenumber, which can be attributed to interactions in the membrane, such as the hydrogen bond between the hydroxyl group of the lactic acid and the carbonyl group of CA. In addition, when the oxygen atom of the carbonyl group newly interacted with the OH groups in the lactic acid, the C=O bond weakened and the peak shifted to a lower wavenumber. However, the area ratio of the 1:0.07 CA/lactic acid membrane at 8 bar was similar to that of the pristine CA, implying that the peak shifted to a higher wavenumber, similar to that of the pristine CA. Since the lactic acid was eliminated by the hydrostatic, the new bond that formed from the interaction between O and H disappeared and the C=O bond strength of the 1:0.07 CA/lactic acid composite at 8 bar recovered to a level similar to that of the pristine membrane. Figure 4 and Table 2 show that the C-O bond and the peak area ratios of the pristine membrane and 1:0.07 CA/lactic acid membrane at 0 bar observed at ~1037 cm^{-1} were 81.54 and 79.24, respectively, and there was no prominent peak shift. Similarly, no significant peak shift was observed between the C-O group of the 1:0.07 CA/lactic acid membrane at 8 bar and that at 0 bar. This implies that the interaction between the lactic acid and CA was more dominant at C=O than at C-O.

TGA was performed to exhibit the thermostability of the membranes. Figure 5 indicates that the 1:0.07 CA/lactic acid membranes at 0 bar had the lowest thermal stability among the three membranes. Upon water pressure treatment, the lactic acid induced a plasticized area in polymer chains, thus increasing the flexibility of the CA chains in that area and the decomposition of the lactic acid. Thus, an irregular collapse was observed in the TGA graph of the 1:0.07 CA/lactic acid membrane at 0 bar in the temperature ranges from 180–250 °C. In contrast, a relatively larger collapse was appeared in the TGA graph of the 1:0.07 CA/lactic acid membrane at 8 bar. This can be attributed to the removal of lactic acid

by the hydrostatic treatment, which eliminated the plasticizing effect of the lactic acid, thus increasing the thermostability of the 1:0.07 CA/lactic acid composite at 8 bar to an almost similar level as that of the pristine CA membrane. In addition, in the TGA graph of the 1:0.07 CA/lactic acid membrane at 8 bar, a slight unusual weight loss was existed in the range 275–300 °C, which can be attributed to the decomposition of lactic acid that remained in small amounts in the chains.

3.3 TGA

TGA was performed to exhibit the thermostability of the membranes. Figure 5 indicates that the 1:0.07 CA/lactic acid membranes at 0 bar had the lowest thermal stability among the three membranes. Upon water pressure treatment, the lactic acid induced a plasticized area in polymer chains, thus increasing the flexibility of the CA chains in that area and the decomposition of the lactic acid. Thus, an irregular collapse was observed in the TGA graph of the 1:0.07 CA/lactic acid membrane at 0 bar in the temperature ranges from 180–250 °C. In contrast, a relatively larger collapse was appeared in the TGA graph of the 1:0.07 CA/lactic acid membrane at 8 bar. This can be attributed to the removal of lactic acid by the hydrostatic treatment, which eliminated the plasticizing effect of the lactic acid, thus increasing the thermostability of the 1:0.07 CA/lactic acid composite at 8 bar to an almost similar level as that of the pristine CA membrane. In addition, in the TGA graph of the 1:0.07 CA/lactic acid membrane at 8 bar, a slight unusual weight loss was existed in the range 275–300 °C, which can be attributed to the decomposition of lactic acid that remained in small amounts in the chains.

3.4 Water flux

The water flux at 8 bar was measured to identify pore information such as the porosity and pore size of various proportions of the CA/lactic acid membrane using a water treatment equipment. The water flux was measured for 1:0.01 CA/lactic acid to 1:0.07 CA/lactic acid mole ratio. The results revealed that the best composition was the 1:0.07 mole ratio, with an average water flux of 5.87 L/m^2h, as shown in Fig. 6. Membranes with a ratio >0.07 showed poor reproducibility, as the lactic acid formed aggregates in the CA membrane.

3.5 porosimeter

A porosimeter was used to examine the porosity and average pore diameter of the CA membrane. The porosity and average pore diameter of the 1:0.07 CA/lactic acid membrane were 65.3% and 0.38 μm, respectively. In a former study, a porous membrane was prepared using an ionic liquid, and the porosity was measured to be approximately 16%.(34) In the case of an ionic liquid, owing to the electrostatic attraction between ions, the viscosity was high, and thus, was unequally dispersed.

In addition, a water channel forms at regions with high concentration of the ionic liquid, thus preventing the even generation of pores, which in turn reduced the porosity. However, due to the relatively low viscosity of the lactic acid, it was well dispersed in the CA. Thus, as shown in Fig. 1, a large number of small pores were formed, resulting in a relatively high porosity and small pore diameter.

4. Conclusion

In this study, we formed lactic acid membranes using a low-cost and pro-environmetal process. The wetting effect of the lactic acid induced plasticization in the CA chain, thus leading to the formation of several micro-size pores in the membrane. The pores which formed on superficies of the membrane were perceived by using SEM, and the SEM images confirmed the formation of sponge-shaped pores in the cross-section of the 1:0.07 CA/lactic acid membrane. In addition, the FT-IR data confirmed the interaction of lactic acid with the C=O group of the CA and showed that the interaction with the C-O groups was more dominant. Furthermore, the TGA data revealed that the hydrostatic treatment removed the lactic acid from the 1:0.07 CA/lactic acid composite and recovered the thermostability of the membrane to a similar level as that of the pristine CA membrane. In addition, the water flux for various compositions was measured to determine the best ratio with the optimal performance and reproducibility. The results revealed that the best composition was the 1:0.07 mole ratio and its average water flux was 5.87 L/m^2h. In addition, the porosity and average pore diameter of the membrane with this composition was 65.3% and 0.38 μm, respectively. Finally, we successfully demonstrated the fabrication of a highly porous membrane using a economical wetting agent.

Declarations

Acknowledgements

This study was supported by the Basic Science Research Program (2020R1F1A1048176) through the National Research Foundation of Korea (NRF), funded by the Ministry of Science, ICT, and Future Planning.

References

1. Basheer C, Alnedhary AA, Rao BM, Valliyaveettil S, Lee HK. Development and application of porous membrane-protected carbon nanotube micro-solid-phase extraction combined with gas chromatography/mass spectrometry. Anal Chem. 2006;78(8):2853-8.
2. Perrotta M, Saielli G, Casella G, Macedonio F, Giorno L, Drioli E, et al. An ultrathin suspended hydrophobic porous membrane for high-efficiency water desalination. Applied Materials Today. 2017;9:1-9.
3. Sajid M, Woźniak MK, Płotka-Wasylka J. Ultrasound-assisted solvent extraction of porous membrane packed solid samples: A new approach for extraction of target analytes from solid samples. Microchemical Journal. 2019;144:117-23.
4. Sulaiman KO, Sajid M, Alhooshani K. Application of porous membrane bag enclosed alkaline treated Y-Zeolite for removal of heavy metal ions from water. Microchemical Journal. 2020;152:104289.
5. Zheng X, Chen F, Zhang X, Zhang H, Li Y, Li J. Ionic liquid grafted polyamide 6 as porous membrane materials: Enhanced water flux and heavy metal adsorption. Appl Surf Sci. 2019;481:1435-41.

6. Esfahani MR, Aktij SA, Dabaghian Z, Firouzjaei MD, Rahimpour A, Eke J, et al. Nanocomposite membranes for water separation and purification: Fabrication, modification, and applications. Separation and Purification Technology. 2019;213:465-99.
7. Fathizadeh M, Xu WL, Zhou F, Yoon Y, Yu M. Graphene oxide: a novel 2-dimensional material in membrane separation for water purification. Advanced Materials Interfaces. 2017;4(5):1600918.
8. Liu M, Song D, Wang X, Sun C, Jing D. Asymmetric Two-Layer Porous Membrane for Gas Separation. The Journal of Physical Chemistry Letters. 2020.
9. Lv J, Gong Z, He Z, Yang J, Chen Y, Tang C, et al. 3D printing of a mechanically durable superhydrophobic porous membrane for oil–water separation. Journal of Materials Chemistry A. 2017;5(24):12435-44.
10. Yu B, Park K, Jang J, Goodenough JB. Cellulose-based porous membrane for suppressing Li dendrite formation in lithium–sulfur battery. ACS Energy Letters. 2016;1(3):633-7.
11. Aboamera NM, Mohamed A, Salama A, Osman T, Khattab A. An effective removal of organic dyes using surface functionalized cellulose acetate/graphene oxide composite nanofibers. Cellulose. 2018;25(7):4155-66.
12. Kalsoom U, Hasan CK, Tedone L, Desire C, Li F, Breadmore MC, et al. Low-cost passive sampling device with integrated porous membrane produced using multimaterial 3D printing. Anal Chem. 2018;90(20):12081-9.
13. Liu H, Hsieh Y. Ultrafine fibrous cellulose membranes from electrospinning of cellulose acetate. Journal of Polymer Science Part B: Polymer Physics. 2002;40(18):2119-29.
14. Matsuyama H, Maki T, Teramoto M, Asano K. Effect of polypropylene molecular weight on porous membrane formation by thermally induced phase separation. J Membr Sci. 2002;204(1-2):323-8.
15. Peng M, Li H, Wu L, Zheng Q, Chen Y, Gu W. Porous poly (vinylidene fluoride) membrane with highly hydrophobic surface. J Appl Polym Sci. 2005;98(3):1358-63.
16. Sun C, Feng X. Enhancing the performance of PVDF membranes by hydrophilic surface modification via amine treatment. Separation and Purification Technology. 2017;185:94-102.
17. Zhang S, Wu L, Deng F, Zhao D, Zhang C, Zhang C. Hydrophilic modification of PVDF porous membrane via a simple dip-coating method in plant tannin solution. RSC advances. 2016;6(75):71287-94.
18. Wang HH, Jung JT, Kim JF, Kim S, Drioli E, Lee YM. A novel green solvent alternative for polymeric membrane preparation via nonsolvent-induced phase separation (NIPS). J Membr Sci. 2019;574:44-54.
19. Adhikari S, Fernando S. Hydrogen membrane separation techniques. Ind Eng Chem Res. 2006;45(3):875-81.
20. Jiang D, Cooper VR, Dai S. Porous graphene as the ultimate membrane for gas separation. Nano letters. 2009;9(12):4019-24.

21. Zhu X, Tian C, Mahurin SM, Chai S, Wang C, Brown S, et al. A superacid-catalyzed synthesis of porous membranes based on triazine frameworks for CO2 separation. J Am Chem Soc. 2012;134(25):10478-84.
22. Pan Z, Cao S, Li J, Du Z, Cheng F. Anti-fouling TiO2 nanowires membrane for oil/water separation: Synergetic effects of wettability and pore size. J Membr Sci. 2019;572:596-606.
23. Qiao Z, Zhao S, Sheng M, Wang J, Wang S, Wang Z, et al. Metal-induced ordered microporous polymers for fabricating large-area gas separation membranes. Nature Materials. 2019;18(2):163-8.
24. Hu M, Yin L, Low N, Ji D, Liu Y, Yao J, et al. Zeolitic-imidazolate-framework filled hierarchical porous nanofiber membrane for air cleaning. J Membr Sci. 2020;594:117467.
25. Yuan S, Li X, Zhu J, Zhang G, Van Puyvelde P, Van der Bruggen B. Covalent organic frameworks for membrane separation. Chem Soc Rev. 2019;48(10):2665-81.
26. Matsuyama H, Maki T, Teramoto M, Asano K. Effect of polypropylene molecular weight on porous membrane formation by thermally induced phase separation. J Membr Sci. 2002;204(1-2):323-8.
27. Gryta M. Influence of polypropylene membrane surface porosity on the performance of membrane distillation process. J Membr Sci. 2007;287(1):67-78.
28. Li D, Shi D, Xia Y, Qiao L, Li X, Zhang H. Superior thermally stable and nonflammable porous polybenzimidazole membrane with high wettability for high-power lithium-ion batteries. ACS applied materials & interfaces. 2017;9(10):8742-50.
29. Nair SS, Mathew AP. Porous composite membranes based on cellulose acetate and cellulose nanocrystals via electrospinning and electrospraying. Carbohydr Polym. 2017;175:149-57.
30. Lagadec MF, Zahn R, Wood V. Characterization and performance evaluation of lithium-ion battery separators. Nature Energy. 2019;4(1):16-25.
31. Lee WG, Cho Y, Kang SW. Effect of Ionic Radius in Metal Nitrate on Pore Generation of Cellulose Acetate in Polymer Nanocomposite. Polymers. 2020;12(4):981.
32. Hong SH, Cho Y, Kang SW. Highly porous and thermally stable cellulose acetate to utilize hydrated glycerin. Journal of Industrial and Engineering Chemistry. 2020.
33. Ertas Y, Uyar T. Fabrication of cellulose acetate/polybenzoxazine cross-linked electrospun nanofibrous membrane for water treatment. Carbohydr Polym. 2017;177:378-87.
34. Lee WG, Hwang J, Kang SW. Control of nanoporous polymer matrix by an ionic liquid and water pressure for applications to water-treatment and separator. Chem Eng J. 2016;284:37-40.

Tables And Scheme

Tables 1-2 and Scheme 1 are available in the Supplementary Files

Figures

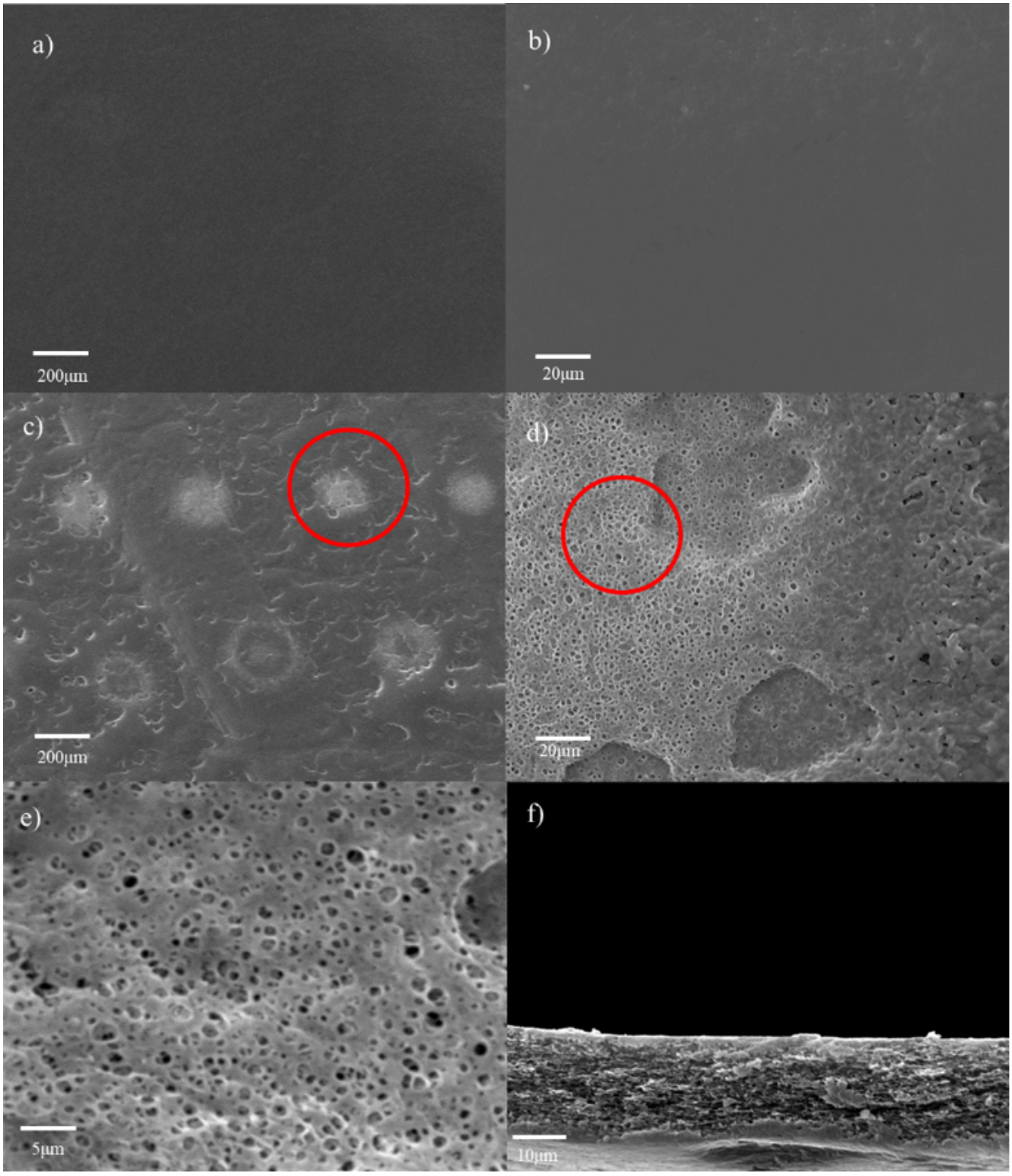

Figure 1

(a) Neat membrane without hydrostatic pressure, (b) 1:0.07 CA/lactic acid membrane without hydrostatic pressure, (c) 1:0.07 CA/lactic acid membrane at 8 bar (magnification ×70), (d) enlargement of (c) (×850), (e) enlargement of (d) (×2,700), and (f) cross-section of the 1:0.07 CA/lactic acid at 8 bar

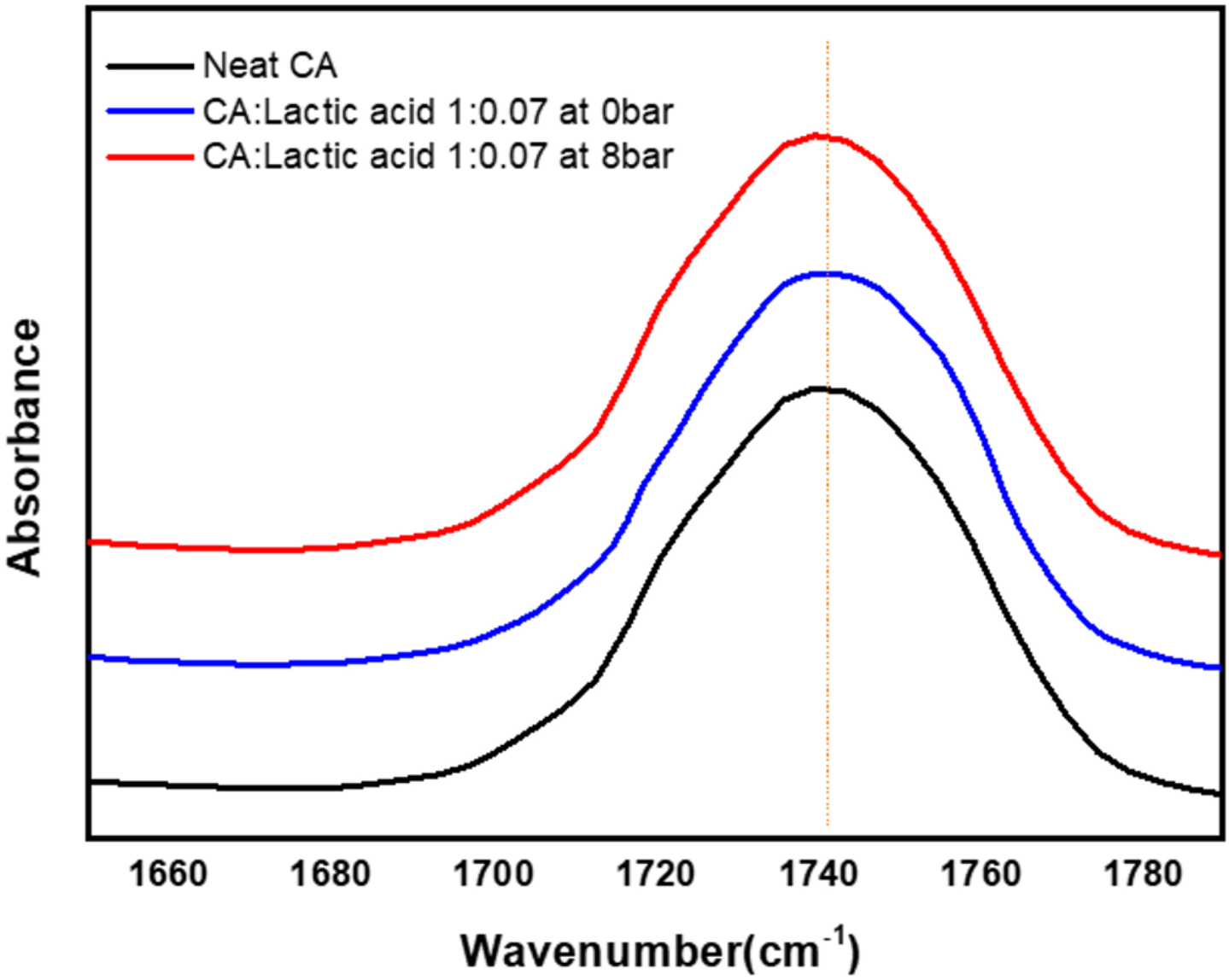

Figure 2

IR data of the neat CA membrane and 1:0.07 CA/lactic acid membranes at 0 and 8 bar.

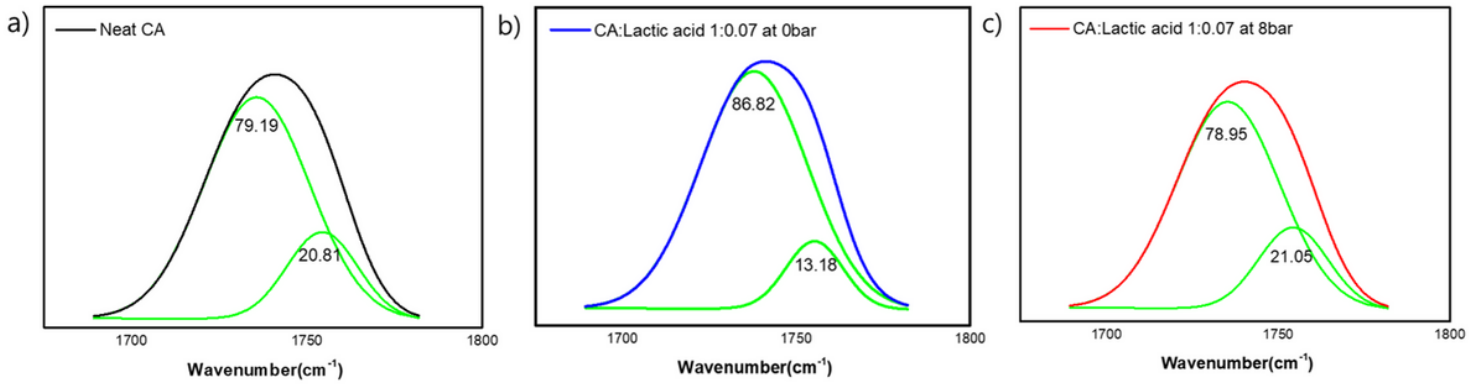

Figure 3

Deconvolution data of (a) Pristine, (b) 1:0.07 CA/lactic acid membrane at 0 bar, and (c) 1:0.07 CA/lactic acid membrane at 8 bar (C=O)

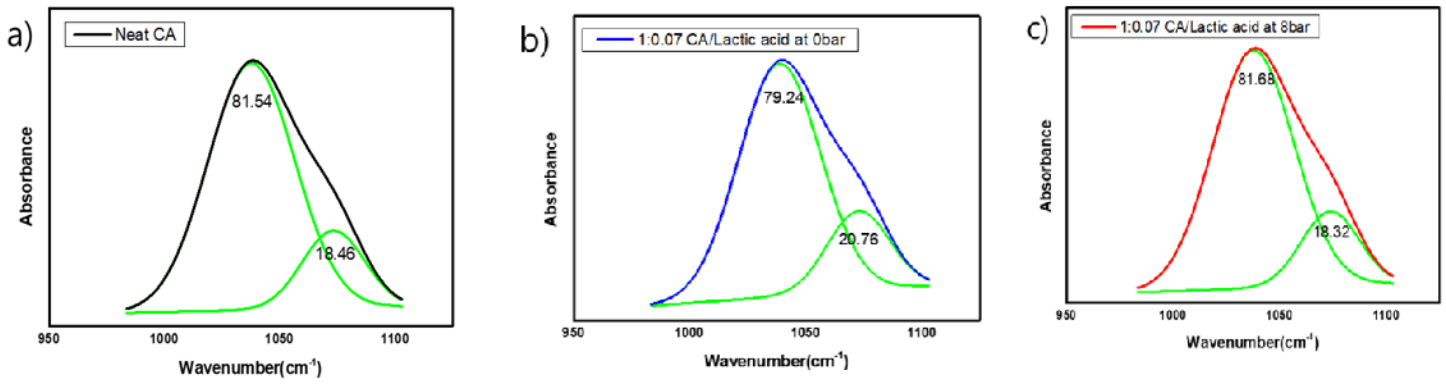

Figure 4

Deconvolution data of (a) pristine, (b) 1:0.07 CA/lactic acid composite at 0 bar, and (c) 1:0.07 CA/lactic acid composite at 8 bar (C-O)

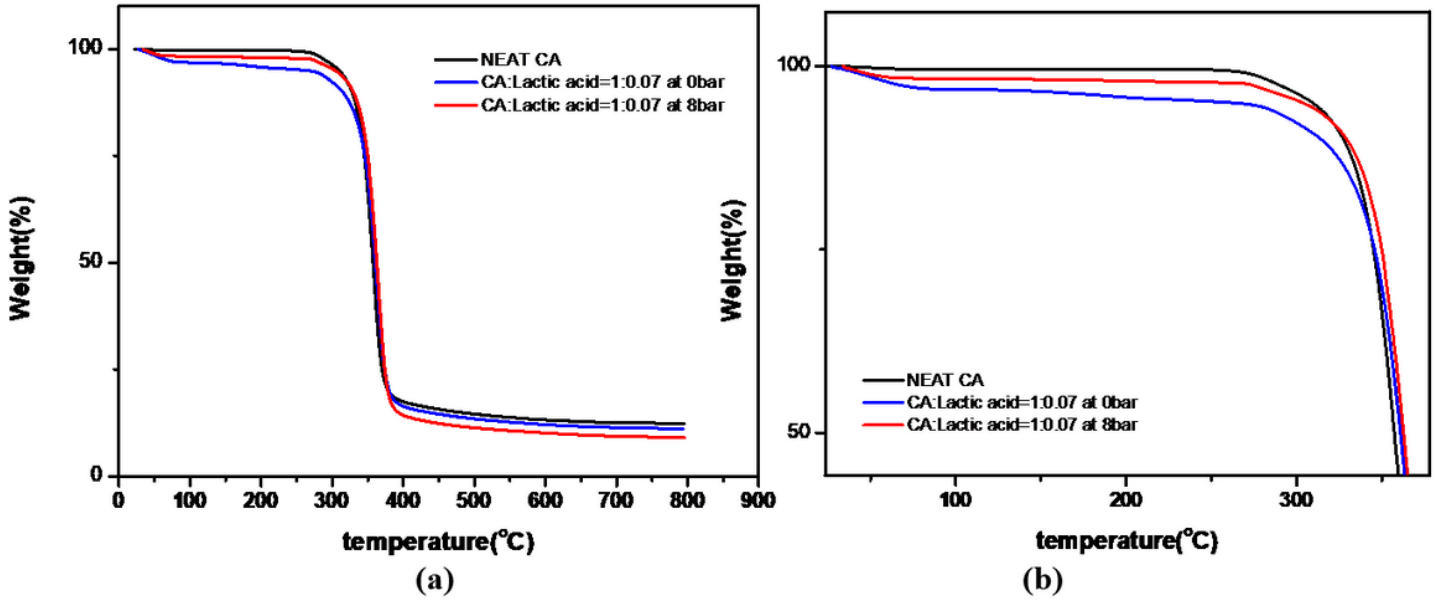

Figure 5

TGA data of (a) Neat CA and 1:0.07 CA/lactic acid membranes at 8 and 0 bar, and (b) enlargement of (a)

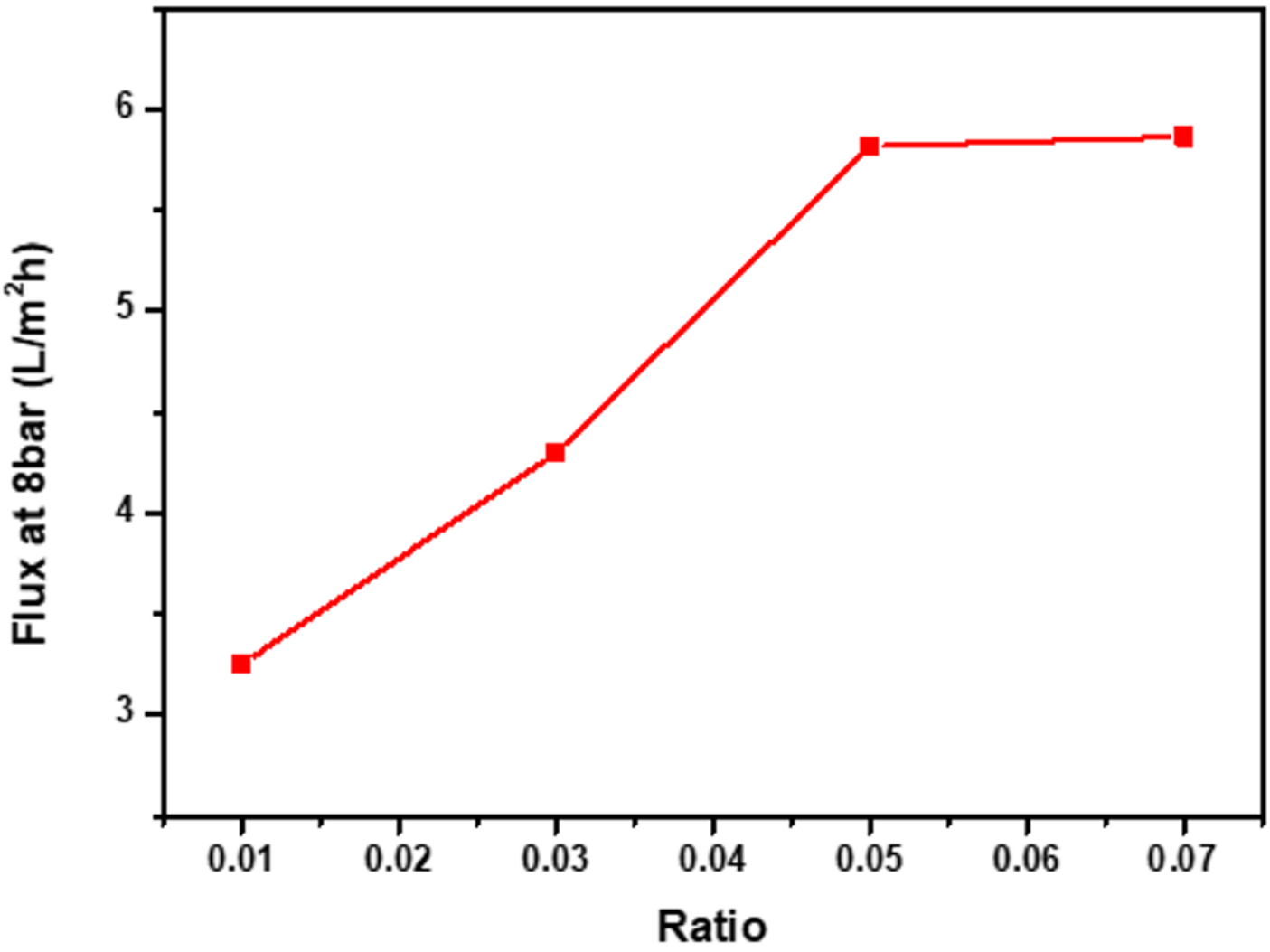

Figure 6

Water flux at 8 bar for various proportions

Supplementary Files

This is a list of supplementary files associated with this preprint. Click to download.

- Scheme1.png
- Tables.docx